Transactions on Engineering and Computing Sciences - Vol. 12, No. 2
Publication Date: April 25, 2024
DOI:10.14738/tecs.122.16645.
Alvarez, R., Camacho, M., & Rivera-Calderón, E. (2024). The Internal Structure of Paricutin and Tancítaro Volcanos, Mexico, From Rock Density Distributions. Transactions on Engineering and Computing Sciences, 12(2). 50-69.

The Internal Structure of Paricutin and Tancítaro Volcanos, Mexico, From Rock Density Distributions

Román Alvarez
ORCID: 0000-0002-2606-0904
Instituto de Investigaciones en Matemáticas Aplicadas y en Sistemas (IIMAS),
Universidad Nacional Autónoma de México, Mexico City 04510, Mexico

Miguel Camacho
ORCID: 0000-0002-3871-6843
Posgrado en Ciencias de la Tierra, Ciudad Universitaria,
Universidad Nacional Autónoma de México, Mexico City 04510, Mexico

Elizabeth Rivera-Calderón
ORCID: 0009-0004-0399-3615
Escuela Nacional de Estudios Superiores-Unidad Morelia,
Universidad Nacional Autónoma de México, Antigua Carretera
a Pátzcuaro 8701, C.P. 58190, Morelia, Michoacán, México

ABSTRACT

Located in the Tarascan plateau, western Mexico, Paricutín volcano is the youngest monogenetic volcano in the country; it is located within 6 km of the only stratovolcano in that region: Tancítaro volcano. The objective is to define the location of Paricutín's magma chamber and the magma conduits constituting its plumbing system. For that purpose, we use a high-resolution, satellite-derived gravity data set to obtain 3D density inversions at two spatial resolutions of 500 and 250 m. Results from the 500 m resolution led us to suspect that a branch of Tancítaro's magma chamber fed Paricutín's eruption; however, at this resolution, we could not find a magmatic path linking them. Results at the higher resolution (250 m) unveiled a channel within a high-density region, in which a vertical, low-density channel is located under Paricutín extending down to 5 km depth, including a region at sea level, that we associate with a small magma chamber owing to its shape and lower density. The volume identified as the magma chamber of Tancítaro volcano is enclosed by a formation of high-density material that appears to have been intruded before the emplacement of the Tancítaro magma chamber; its nature and composition cannot be determined with the available information.

Keywords: Tancítaro volcano, Paricutín volcano, Magma chamber, Satellite-derived gravity, 3D gravity inversion.

INTRODUCTION

Paricutín volcano, in the western state of Michoacan, is the youngest volcano in Mexico, it was born on 1943-2-20, destroying the town of Parangaricutiro; there is ample information about its birth and evolution, including geologic descriptions, seismic records, photographs, and even

motion pictures. Here we look at the volcano's interior to locate and describe the magma source that provided the extensive lava flows that were extruded at the base of the volcano. Initially, [1] described the composition of the lavas as monotonously uniform olivine basalt; however, recent studies report variations in the lava classification ([2]. Using progressively higher-resolution 3D inversions, we identify the magma chamber and the plumbing system through which lavas were erupted, within a high-density formation surrounding the magmatic chamber of Tancítaro volcano (TV). According to [3], TV became active at ~800 ka, with the most recent effusive activity at ~240 ka. We explore the origin and evolution of Paricutín and its relation to the evolution of TV; the best way to understand its behavior is by analyzing both structures simultaneously.

Paricutín belongs to the Michoacán-Guanajuato volcanic field (MGVF) and as already mentioned, is quite close to the major volcanic structure in the area: Tancítaro volcano. According to [4], the MGVF contains 1040 volcanoes, most of them cinder cones, shield volcanoes, maars, lava domes, tuff rings, and cone-less lava flows, in an area of 40,000 km2. The cinder cone density is highest in the Paricutín area (141 vents in 1250 km2). They mapped the alignment of cinder cones ≤40 ka, with Paricutín the youngest, finding a group orientation close to azimuth 45º. It is convenient to recall that the second most recent volcano in this region was born 77 km SE of Paricutín, called El Jorullo, in 1759. The Tarascan plateau (Figure 1) is located at over 2000 m elevation and contains many volcanic structures, one of them Paricutín itself. Seismic activity in the area is widespread [5] [6] [7].

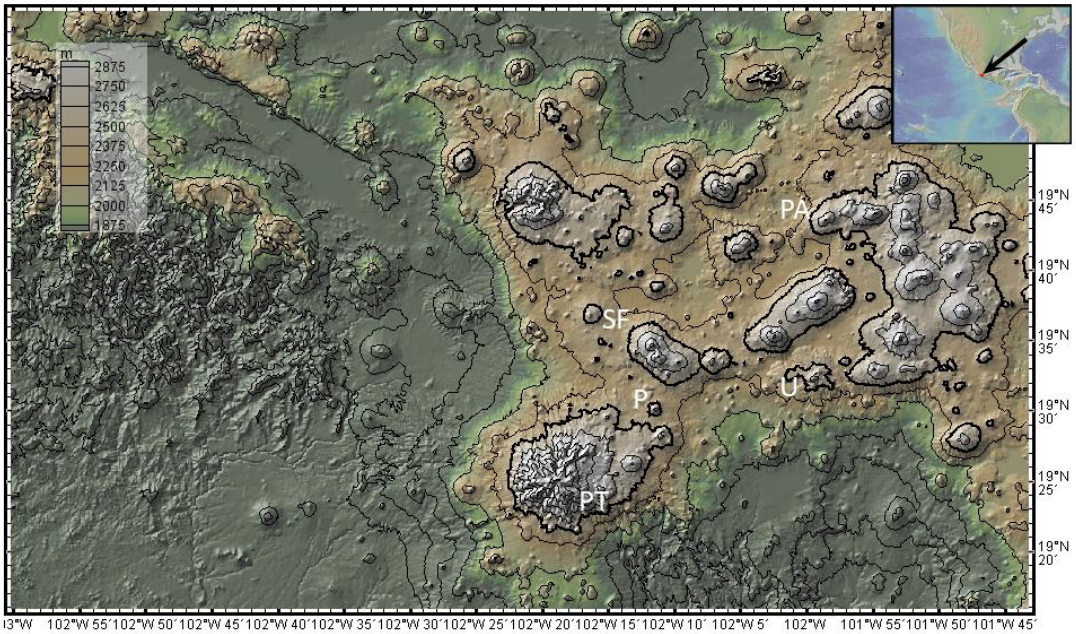


Fig.1: Topography of the Meseta Purépecha (brown tones), also known as Tarascan Plateau, showing elevation contours. The elevation of the plateau is >2000 masl and is heavily populated by volcanic structures. P, Paricutín. PT, Tancítaro volcano. U, Uruapan. PA, Paracho. SF, San Francisco. Topographic map from GeomapApp.

GEOLOGICAL SETTING

The Trans-Mexican Volcanic Belt (TMVB) is a continental volcanic arc resulting from the subduction of the Cocos and Rivera Plates at the Middle American Trench (MAT), along the central portion of Mexico, in an E-W direction ([8] [9]. This peculiar geometry suggests a fragmentation of the Cocos plate with different inclinations for each of the fragments that subduct under the North American plate [10]. This complex geometry of the oceanic slab has given rise to a great variability of volcanic styles and the chemical composition of its products [11] [12] [13].

Paricutín volcano is the youngest structure in this field and one of the most studied in the world. It was born in 1943 and its activity ended in 1952. In the 10 years of activity, it generated an approximate volume of 1,754 km^3 of lava covering an area of 25 km^2 [8] [14] [15].

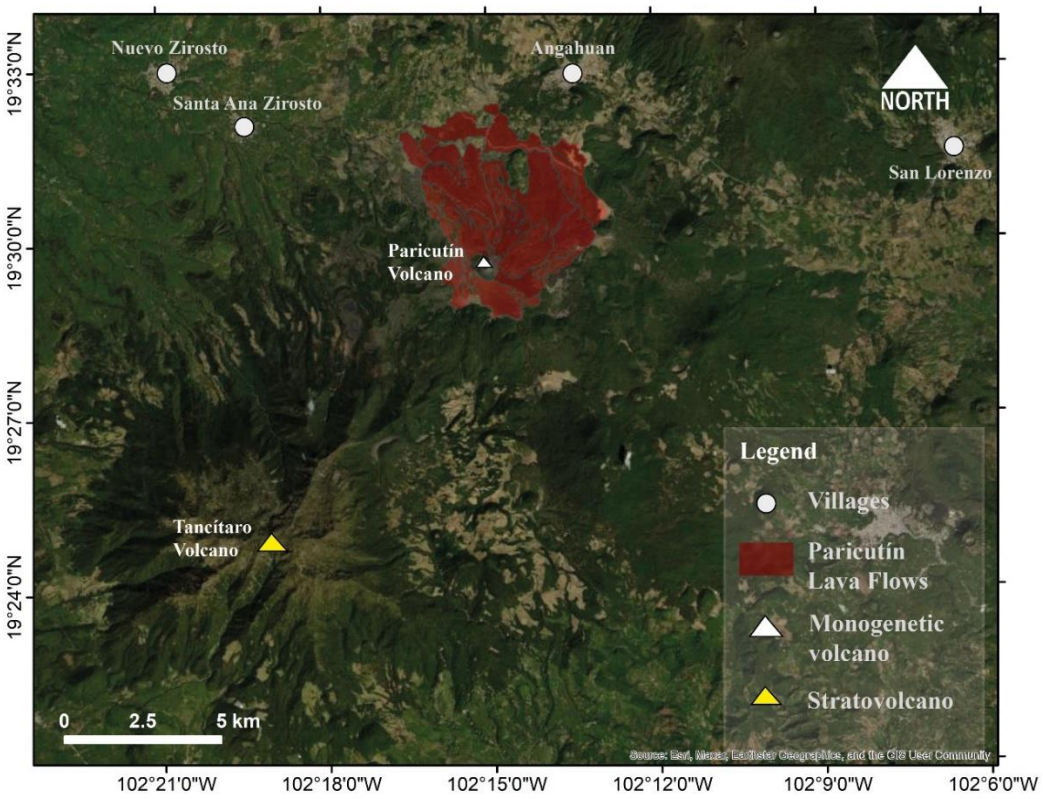


Fig. 2: Local map showing Tancítaro stratovolcano and the Paricutín structure. The villages are labeled, and the red polygon shows the distribution of the Paricutín lava flows.

Paricutín and the volcanic structures of this volcanic field are emplaced and oriented by regional tectonic directions [8]. The two main trends are NW-SE of the Tepic-Chapala rift valley and NE-SW of the Miocene to present-day normal fault system [8] [16]. Paricutín represented a study opportunity for geologists and specialists from around the world, who recorded the evolution of the birth of the volcano [17]. Its activity was divided into four stages: the first stage (February 20 to October 18, 1943), consisted of recurrent lava flows, the intermittent eruption of pyroclastic material, mainly bombs and lapilli. During this period, the growth of the volcano

was accelerated, and the cone would reach slightly over 300 m in height, representing 75% of the total height. Despite its short duration, the second stage (October 18 to January 8, 1944) was characterized by the abundance of extrusion of lava flows to the north. During this time, smaller volcanic conduits emerged, called Mesa del Corral, Sapichu, and Ahuan; they are oriented in an east-northeast direction. A surface geophysical study is available [18].

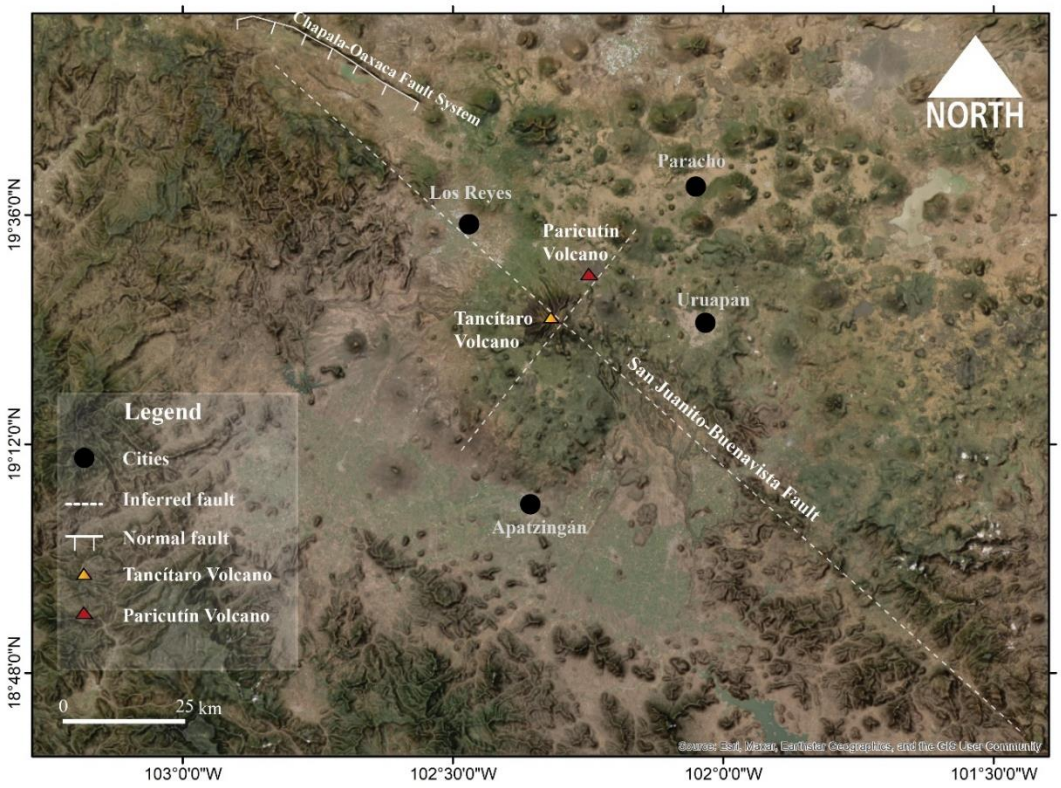


Fig. 3: Location of Tancítaro stratovolcano and Paricutin monogenetic volcano, main cities, inferred faults and normal faults are included. The spatial distribution of the inferred faults was assembled from geomorphology and published sources [19] [7] [5].

The volcanic activity of these cones, mainly Sapichu ("Child" in Purépecha dialect) was of a Strombolian type, although smaller than the main cone. The lava spills covered an approximate extension of 3.5 km. In the third period (January 8, 1944, to January 12, 1945), a series of cracks formed south of the main cone, known by geologists as the Taquí and Ahuan volcanic conduits period. During this period there was an activation of the main cone, which produced lava flows that reached their maximum distance to the west and northwest. The flows reached 10 km covering an area of 17 km^2. Figure 2 shows the lava extent in the vicinity of Paricutín. San Juan Parangaricutiro was completely evacuated, and the main cone reached its maximum height of 355 meters. The fourth and last period was characterized by long periods of calm and lapses of pyroclastic flows and ash activity. It finally ended its activity on March 04, 1952 [20] [21] [17]. The spatial distribution of faults appears in Figure 3, showing their relation to Tancítaro and Paricutín volcanoes.

Subsequently, the lavas and pyroclastic products were analyzed by geochemical studies that suggest that the main mechanism that originated the lavas was of the assimilation type by fractional crystallization in a calc-alkaline environment [15], which evolved by possible fractional crystallization and cortical contamination of the granitic basement according to evidence of xenoliths studied in the region [16] [17].

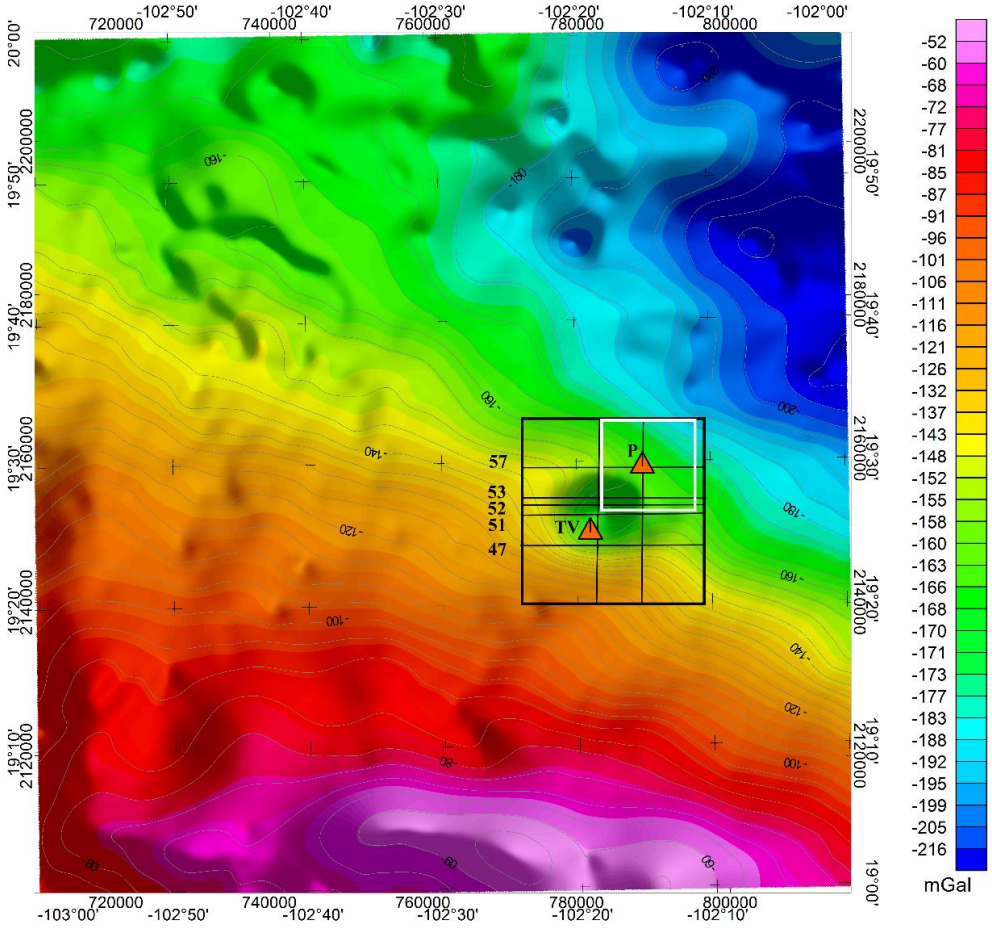


Fig. 4: GGMplus Bouguer anomaly (BA) map of the Tancítaro-Paricutín region and its vicinity. The black rectangle is an approximately 25 x 25 km² region in which a 3D inversion is completed; it includes TV and Paricutín locations. Black lines within the rectangle (5 horizontal and 2 vertical) represent the location of E-W, 0.5 km resolution, density cross-sections extracted from the inverted volume and referred to in the text as L_2147 through L_2157; similar, N-S cross-sections are indicated through TV and P. The white rectangle is a 12.5 x 12.5 km² region centered on the Paricutín location; the corresponding 3D inversion has a resolution of 250 m. Gravity contours are thin, black lines.

GRAVITY DATA

High-resolution gravity data were obtained from the GGMplus repository as Gravity Observed in the Surface (http://ddfe.curtin.edu.au/gravitymodels/GGMplus/) with a resolution of 7.2 arc-sec (200 m) [22].

The elevation model used for the calculations was the Digital Elevation Model (DEM) SRTM90, with a 7.2 arc-sec resolution (The NASA Shuttle Radar Topographic Mission; https://srtm.csi.cgiar.org/srtmdata/; [23].

From the observed gravity data (G_Obs), we performed the calculation of the Bouguer Anomaly (BA) including the necessary corrections according to the new gravimetric standard of the USGS, e.g., [24]. Detailed steps for the BA computation are described in [25] [26] [27].

Bouguer Anomaly

A general discussion is made of the characteristics of the BA in the Tancítaro-Paricutín region (Figure 4). The BA map shows values ranging from -52 to -223 mGal. A strong decreasing gradient of the BA in the SW-NE direction is observed. The highest anomaly is found in the central-southern region of the map, extending from W-E, while the lowest anomalies are in the NE region of the map, extending in an N30°W direction.

The rather uniform behavior of the gravity contours in the region appears heavily distorted around the negative anomaly associated with the Tancítaro volcano. Between Paricutín and Tancítaro volcanos there is an abrupt change in the anomaly contours, which are oriented perpendicular (N30°E) to the regional trend of the AB contours. This results in an extraordinary, regional anomaly minimum located between Tancítaro and Paricutín; this minimum will be further explored when the 3D gravity inversion is performed.

In the NW portion of the map, the gravity gradient decreases and appears to give rise to a large distribution of low-gravity anomalies, which would in turn facilitate intrusion emplacements, some of which are located close to the surface. This interpretation is in line with the intense seismicity observed in the area, e.g., [7] [6].

3D Inversion

The result of a gravity 3D inversion of the area covered by the black rectangle in Figure 4 is shown in Figure 5. This is a rectangular volume in which a successively adjusted density distribution reproduces the observed gravity field, within imposed error limits. Gravity inversions transform gravity distributions, in mGal, into density distributions, in g/cm^3. The inversion process associated with volcanic structures has been discussed in [28] [25] [26] [27]; the reader is referred to these publications for details about the inversion process.

Gravity Cross-Sections

Seven density cross-sections will be discussed about the volcanic structure of Paricutín and its connection with Tancítaro volcano (see Figure 4). Lines 2147-2157 have a resolution of 0.5 km and up to 7 km depth, showing in detail the plumbing system of TV and a branching low-density region that we identify as the Paricutín Branch.

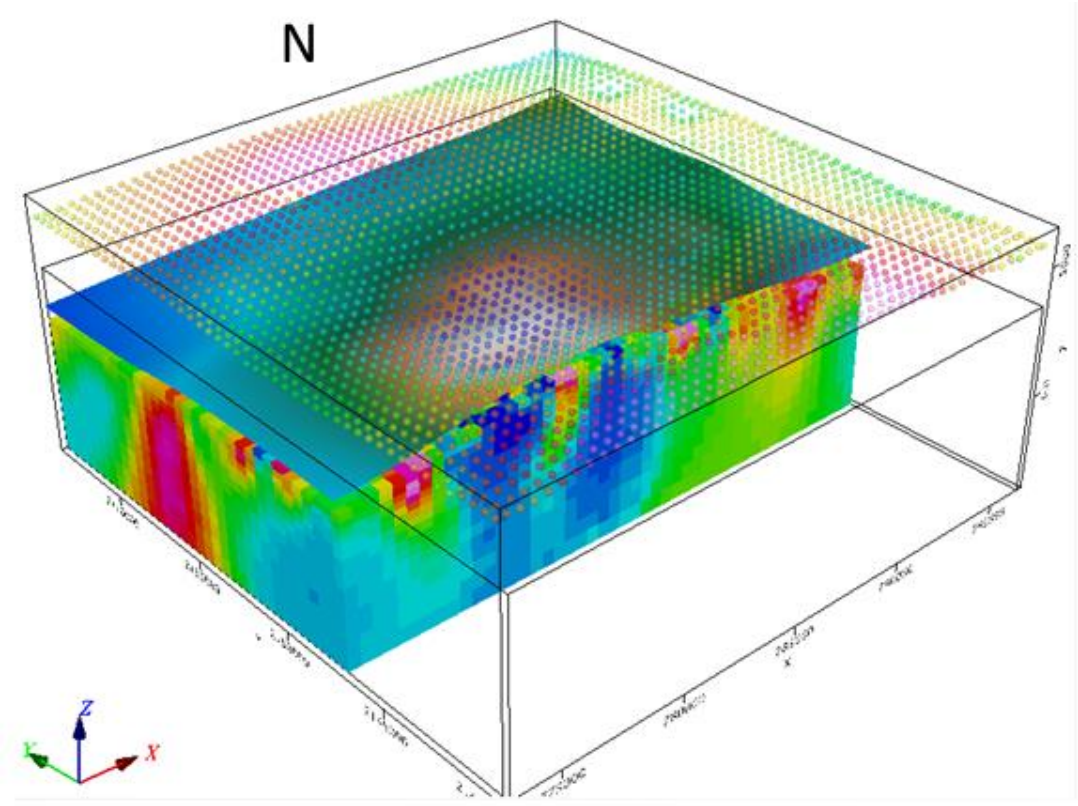


Fig. 5: Inverted density volume (25 x 25 x 5 km³) showing from top to bottom: i) the colored dots represent the location of the gravity stations used in the inversion, ii) a partial view of the DEM, and iii) a vertical, E-W plane passing through TV, showing two low-gravity anomalies associated with it, reaching the bottom of the model. Density cross-sections will be derived from this volume and will be discussed ahead.

L_2147

The location of this density cross-section appears in Figure 4, it has a resolution of 500 m and was extracted from the 3D inverted, density volume. The model elevations are averaged at 500 m intervals; the highest section corresponds to the largest elevation of TV, at its center there are a high-density region flanked by two, neatly defined, low-density regions that continue downward to the bottom of the model, at -3000 m below sea level (bsl). They are the two branches ostensibly being fed by a deeper magma source. We shall name them, the western and eastern magma chambers.

The western magma chamber (Figure 6) extends from -2 km bsl to the surface, or a length of ~4 km in a rather wide conduit of ~2 km that shows a minimum close to the surface (1.5 km asl). A central low-density region located between sea level and 2500 mbsl appears to feed the western and eastern magma chambers, in turn being fed by a deeper magma source with a conduit, not a magma chamber, located at -4000 mbsl. The eastern magma chamber shows a minimum at sea level with conduits extending from 3 km bsl to the surface; it shows a bulge to the E connecting close to sea level to a branch rising at a ~45º angle towards the E. This branch is a surficial, low-density region close to, but south of, Paricutín volcano. At the Eastern Branch,

the lowest density is quite close to the ground surface, as in the eastern and western magma conduits of Tancítaro volcano.

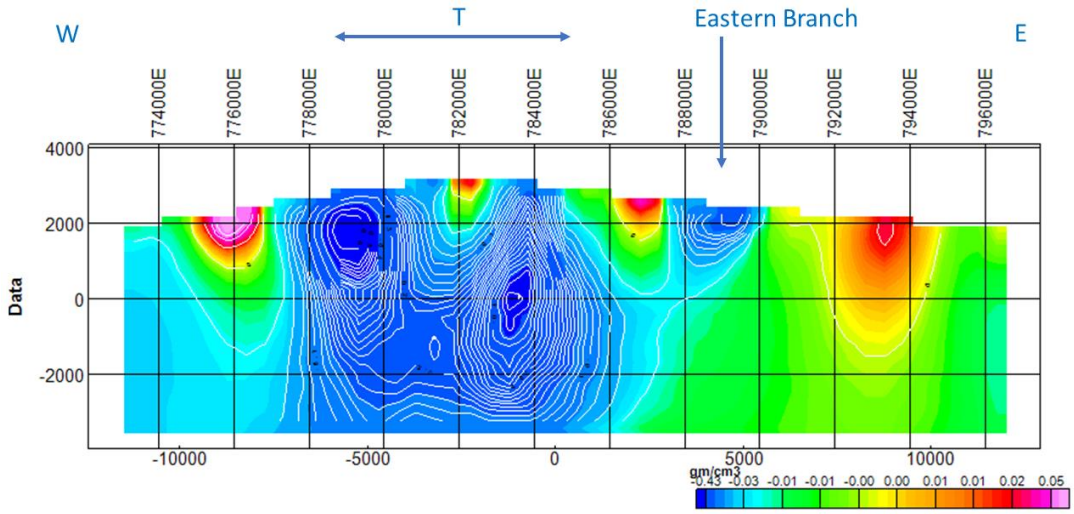


Fig. 6: The cross-section L_2147 runs E-W; it has a resolution of 500 m. Topography is averaged to this resolution. Negative anomalies predominate under Tancítaro volcano (T); several minima are identified as deposits of eruptive materials or magma chambers with corresponding conduits reaching the surface. An adjacent anomaly to the E corresponds to the Eastern Branch. Add 2.67 g/cm^3 to the scale values to obtain actual density values.

L_2151

This E-W trending line is parallel to, and 4 km N of, L_2147 and is shown in Figure 7. The deep connection between the low-density regions of TV and the named Eastern Branch is more clearly shown; a chimney of TV is defined at 782000E, whilst flanking it on the eastern side of the summit, a low-density pocket is observed. The lowest density value under the Eastern Branch is located at +1800 masl suggesting it is the location of the shallow magma reservoir from which lavas were expelled to the surface, giving rise to the unnamed cinder cone shown in the topographic profile. The equivalent lowest density region of TV is located at 1 km bsl, extending downward in the E direction (i.e., towards Paricutín).

L_2152

This E-W trending line is parallel to, and 5 km N of, L_2147 and appears in Figure 8. The distortion towards the E of the low-density region, continues as observed in Figure 7, although it is of lesser intensity, indicating that the border of the low-density region is being approached. The connection with the Eastern Branch persists, although with a tendency to disappear. Two high-density sections flank the low-density region separated by ~25 km.

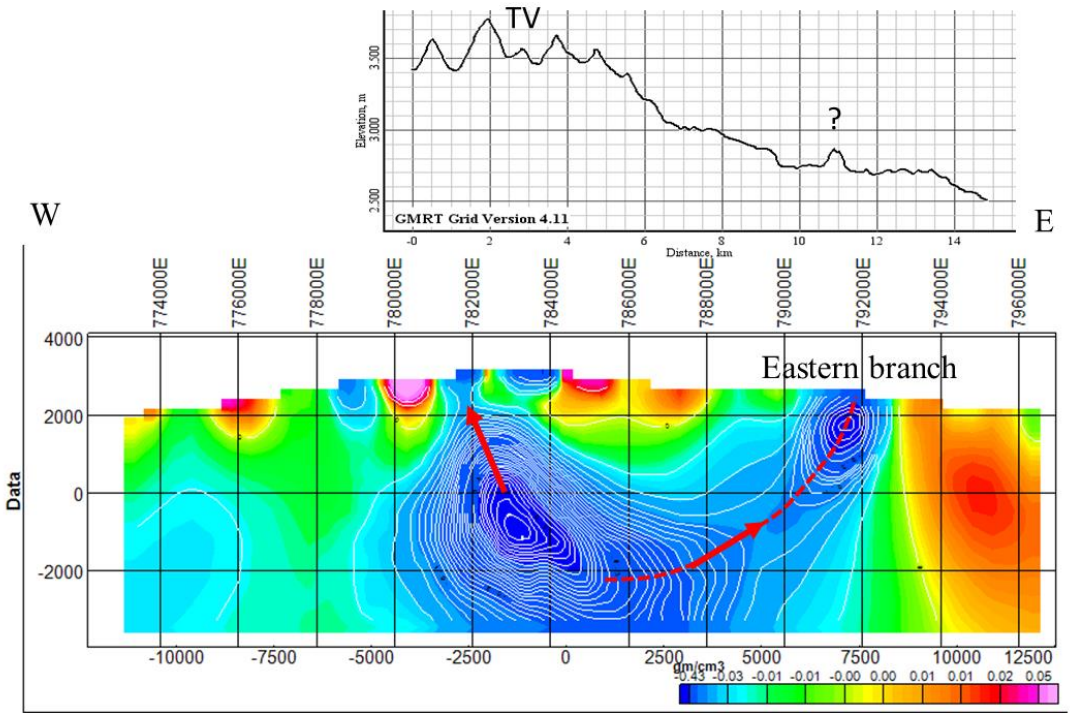


Fig. 7: Density cross-section along L_2151 showing the displacement towards the E of magmatic materials from the chamber of Tancítaro volcano (TV), also showing a chimney at 782000E. The magma conduit connection with the Eastern Branch is more clearly defined, showing a quite superficial magma deposit of that branch, located slightly below the +2000 m elevation, and confirming that feeding of this chamber occurred at an approximate angle of 45º, from a depth close to 2000 mbsl. Red arrows show the inferred flux direction of magmatic products. A volcanic cone, whose name (?) could not be determined, is present in the associated topographic profile. Add 2.67 g/cm³ to the scale values to obtain actual density values.

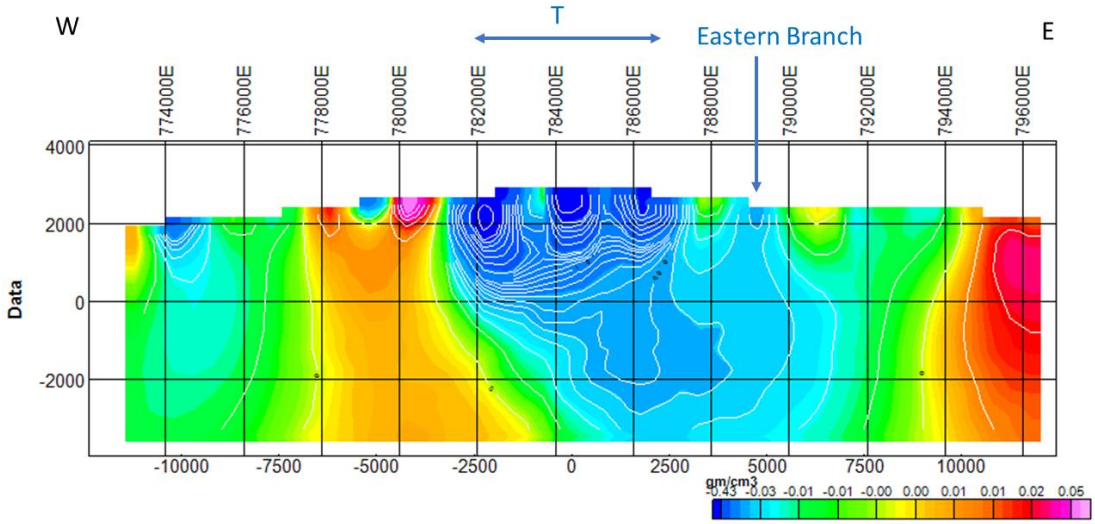


Fig. 8: Density cross-section along L_2152 showing the distortion towards the E of the magma chamber of TV and three surficial low-density regions that appear to have alternated as

chimneys of TV. The Paricutín connection is fainter but clearly defined. Add 2.67 g/cm³ to the scale values to obtain actual density values.

L_2153

In the transition between L_2152 and L_2153, the presence of a small magma chamber appears centered at 500 masl, of the Eastern Branch, with two conduits reaching the surface (Figure 9); it is worth noticing the geometric difference between the Paricutín branch in these two lines, since in the former there is no density minimum associated with it, whilst in the latter such a minimum is well defined. Regarding the conduits in L_2153, the one W of the chamber is associated with the TV summit, whilst the conduit E of the chamber is in the Eastern Branch; Paricutin's cone is approximately 4 km to the N of this location. The flanking, high-density regions become more prominent.

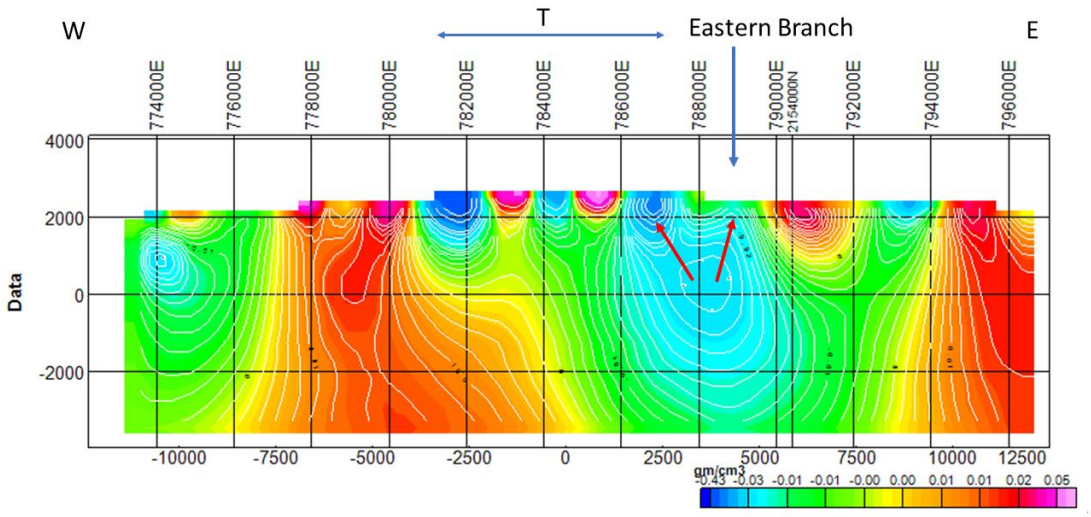


Fig. 9: Density cross-section along L_2153 showing a low-density region displaced eastward from the summit of TV. We identified the region of the lowest density with the magma chamber that fed surficial discharges southward of Paricutín volcano. Two red arrows depict discharge trajectories toward the surface. Add 2.67 g/cm³ to the scale values to obtain actual density values.

L_2157

Line L_2157 goes across the Paricutín summit (Figure 10) showing a shallow, low-density patch with an estimated thickness of 1.4 km. The peculiarity of the density cross-section in Figure 10 is the extended presence of high-density materials, contrasting with the formerly displayed cross-sections dominated by low-density materials; this is an unexpected result. The contours and colors of the density values in L_2157 help visualize what we interpret as an abandoned magma chamber, where its central portion was located at -3000 m elevation with extensions to the E and W; the E extension surfaces at Paricutín location whilst the W one remains at depths similar to that of the magma chamber. There is still a third one, extending from the abandoned magma chamber to the surface at 78100E.

The geometry, distribution, and depth of the highest-density distributions are like the low-density distributions in L_2147 and L_2151. A possible explanation for the existence of this anomalous distribution is that, while it was active it was being fed by magma conduits that were eventually blocked stopping the supply and initiating a cooling process in which the low-density materials were progressively converted into high-density ones. One is tempted to associate the high-density regions with the granitic basement; however, this is speculative since at this point, we do not have the needed information to confirm it.

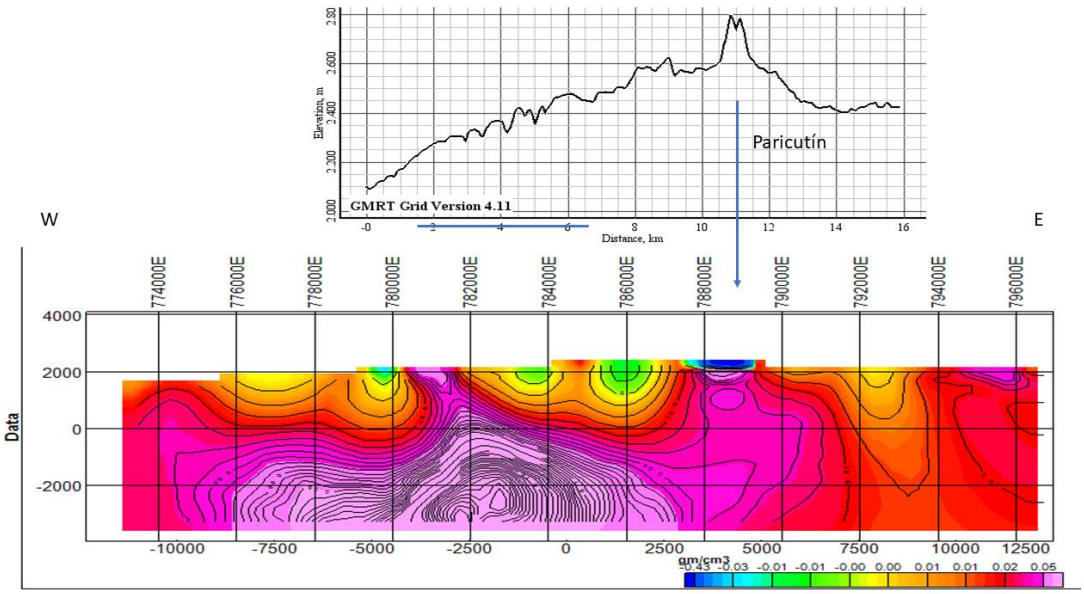


Fig 10: Density cross-section along L_2157 with a resolution of 0.5 km. On top is the topographic profile at 30 m resolution; horizontal scales are equal, and eastings are matched. Paricutín corresponds to the surficial, lowest density anomaly; the cross-section in the cross-sections shows a wide, high-density region that appears to be solidified, apparently the site of a once magmatic chamber between 2-3 km bsl, with a branch towards Paricutín. Add 2.67 g/cm^3 to the scale values to obtain actual density values.

There is a definite association between this low-density region under Paricutín volcano and its eruption materials. However, the question arises regarding the direction from which the low-density region was fed, since it is on top of a high-density one; we originally assumed that lateral feeding in the N-S direction was a possibility, proceeding to obtain the corresponding N-S cross-section, shown in Figure 11, exhibiting also a low-density anomaly on top of a high-density region. Since the E-W and the N-S cross-sections show the low-density anomaly over the high-density region, creating an apparent inconsistency, we questioned how this material, apparently associated with Paricutín volcano reached that location.

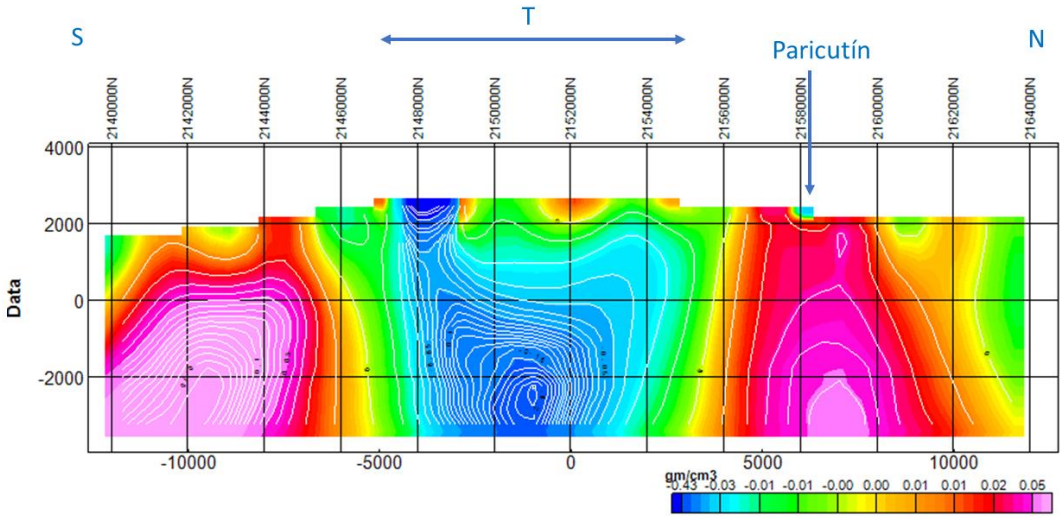


Fig. 11: N-S density cross-section through TV and Paricutín. Resolution 0.5 km. The TV low-density anomaly extends from top to bottom of the cross-section, whilst the low density associated with Paricutín rests upon a high-density region. The two high-density regions constrain the low-density anomaly of TV. Add 2.67 g/cm^3 to the scale values to obtain actual density values.

To further explore the origin of this apparent inconsistency, we extracted a horizontal section at sea level at the 500 m resolution (Figure 12) and obtained a geosurface (Figure 13) that locates a volume of lower densities; both help understand the distribution of materials in this area. Most cross-sections at 500 m resolution (Figures 7-11) showed high-density regions constraining the low-density ones. Figure 12 shows that at sea level there is an almost circular, high-density region enclosing the low-density anomaly of TV; crossed lines show the Paricutín location, just at the border of the high-density region and close to a vertical zone to the E in which the circular density pattern decreases. The higher resolution (250 m) of the vertical cross-section in Figure 14 confirms this distribution at sea level, revealing that this is the most likely region through which the Paricutín eruption was supplied.

GEOSURFACE

A geosurface is a surface that encloses rocks of densities lower than a given density value; Figure 13 shows the geosurface whose value is 2.62 g/cm^3; the interior of the geosurface contains densities below that value. It was chosen since it complements other cross-section views indicating the present distribution of low-density regions in TV and Paricutín. There is the main geosurface and several other, smaller geosurfaces dispersed around the volume. As noted above, we associate low-density regions with the presence of magmas and the conduits that transport volatiles. Comparison of the 2D cross-section of L-2151 (Figure 7) with the 3D geosurface geometry helps understand the role of the geosurface. As expected, the geosurface and the 2D cross-section coincide in the definition of the path of the lavas and volcanic products that give rise to the Paricutín Branch. Other conduits defined by the geosurface also reach Tancítaro's surface; a detailed discussion of those features is not the purpose of the present work, and they will be examined elsewhere.

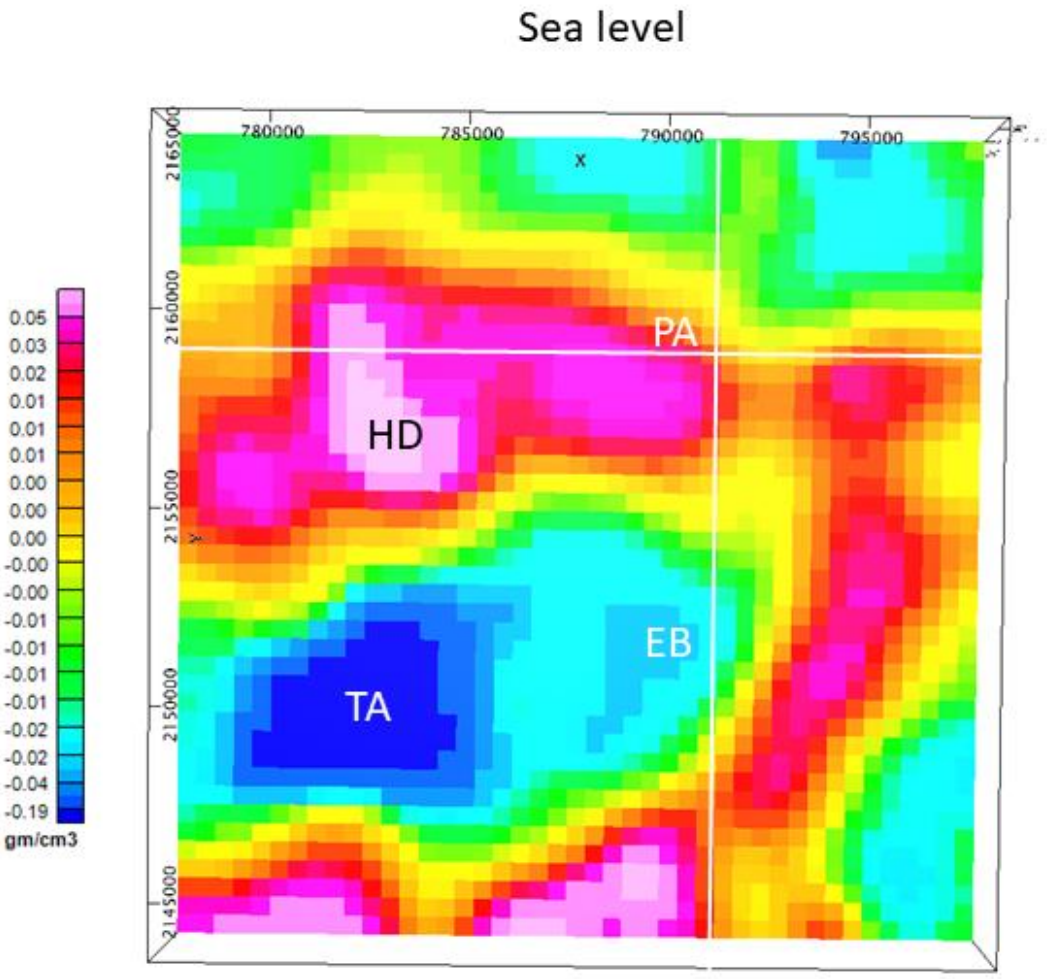


Fig. 12: Horizontal section at sea level, extracted from the 3D gravity inversion at 500 m resolution; Paricutín location is at the crossing of the two white lines (PA) on the NE border of the high-density region, that in turn contains a region to the W of higher-density (HD). TA, Tancítaro low-density anomaly; EB, Eastern Branch. The location of Paricutín in the rim of a high-density region is an unexpected experience since magma chambers and the associated conduits are usually linked with low-density distributions.

We selected to perform an additional 3D inversion of the Bouguer anomaly at a higher resolution, to verify whether this could help identify the conduit that fed Paricutín's eruption. Figure 14 shows the vertical cross-section obtained along Paricutin's location with a resolution of 250 m. The new inverted region is the white rectangle in Figure 4, at half the size (12,500 m) of that used to obtain the cross-sections in Figures 6-12, and consequently double its resolution. A cross-section obtained from this inversion across Paricutín is shown in Figure 13, where two channels within the high-density region predominate on its eastern portion below +1000 mbsl, presenting a vertical, internal, elongated lower-density section, which we interpret as the conduit of the magmatic materials that induced the Paricutín eruption. At the 500 m resolution, these density regions are averaged with the neighboring ones, and thus cannot be discerned.

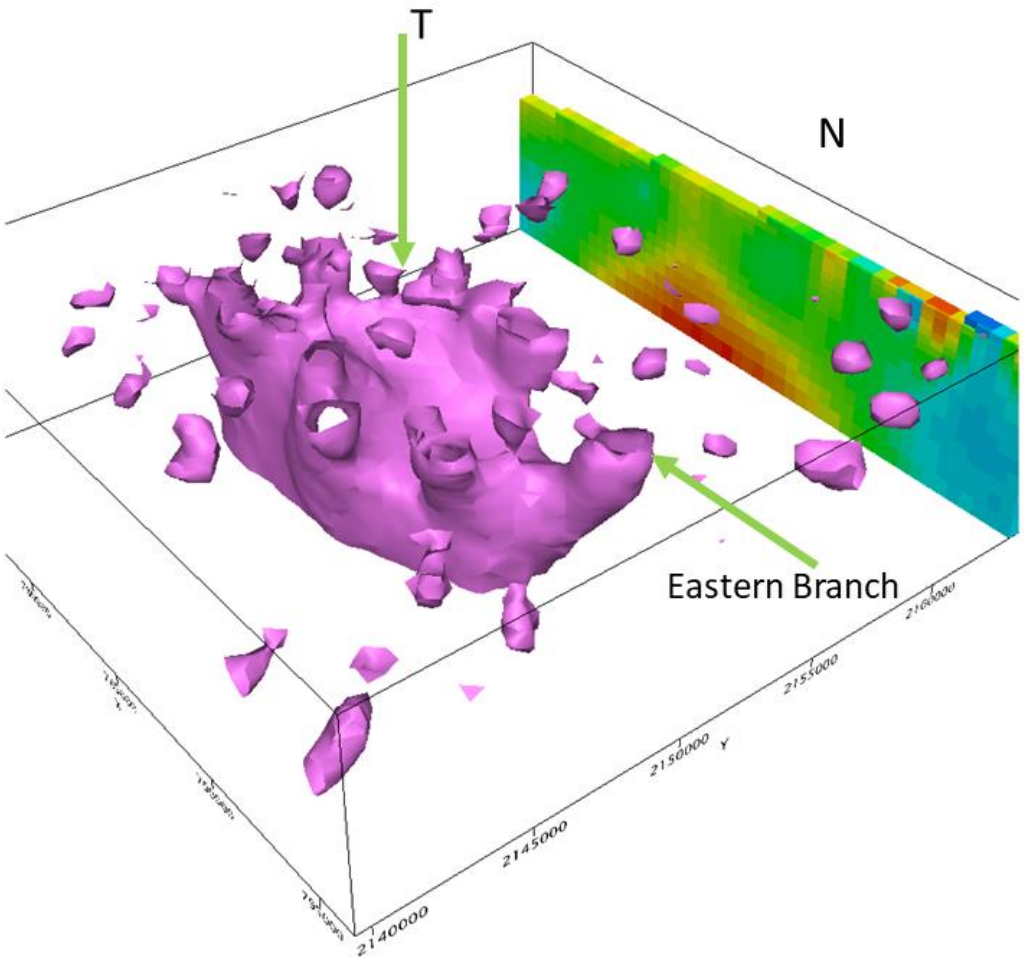


Fig. 13: Geosurface (magenta) derived from the 3D inversion, enclosing densities ≤2.62 g/cm³ helping visualize the 3D distribution of low-density components; the main body of the geosurface corresponds to Tancítaro volcano (T), several branches are reaching the surface, one of them corresponds to the Eastern Branch feeder (see Figure 7). The model resolution is 0.5 km.

Given the shape and dimensions of the eastern conduit, it appears viable to consider the low-density region at sea level as a magma chamber; however, it is worth noticing that the presence of low-density channels within high-density materials is not a common observation. To verify this trajectory, we proceeded to analyze the vertical evolution of the low-density region, as shown in Figure 15.

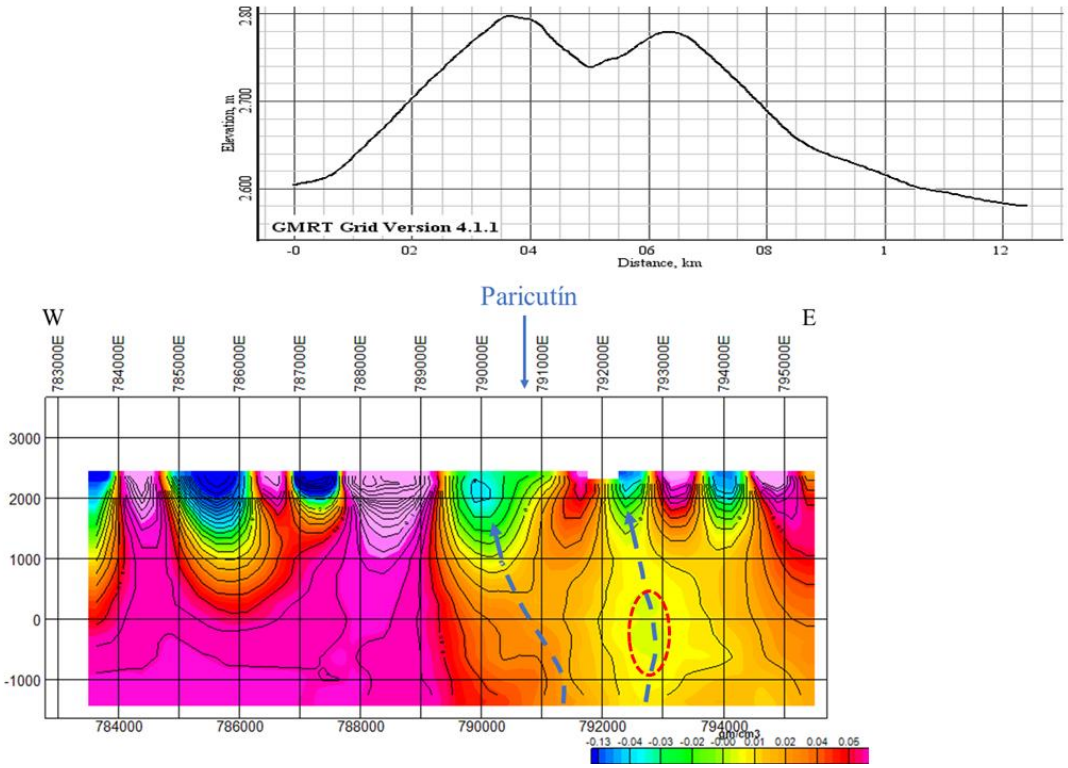


Fig. 14: L_2158 has double the resolution (250 m) of L_2157; above, the topographic profile of Paricutín, the horizontal scales are equal. On the western half of the cross-section high-density formations predominate, whilst on the eastern half medium-density formations are located. At this scale, two possible paths are shown as dashed lines, of magmatic materials feeding Paricutín. The E path shows a minimum-density region centered at sea level (red dashes), which appears to be the most likely location of the magma deposit that fed Paricutín.

Figure 15 contains six horizontal sections at elevations ranging from -1500 m to +2000 m, where the location of Paricutín volcano is marked as the intersection of two white lines. At the deepest section (-1500 m), the Paricutín is located at the border of the high-density region. The section at -750 m elevation shows that the highest-density region experiences a small size increment, whilst Paricutín remains at the border of that region. At sea level (0 m elevation) Paricutín's location is occupied by a slightly less dense region that increases in size at the +750 level, density decreasing again at +1500 and +2000 masl. On the surface, there is a fragmented anomaly landscape. Thus, the vertical cross-section in Figure 12 properly displays the low-density trajectories (dashed lines) inferred from the horizontal section sequence in Figure 15. In summary, Paricutín's eruption appears to have been fed from a small magma deposit located at sea level, showing a modest low-density region in the neighborhood of a massive high-density region.

Visualizing the density distribution of high- and low-density materials under the two volcanoes proved to be difficult; to aid in this task we prepared two conceptual models that appear in Figure 16 along an E-W orientation. The model corresponding to Tancítaro emphasizes the low-density magma chamber that feeds various conduits reaching the summit of the volcano, as well

as a major magma migration that we identified as the Eastern Branch, feeding an unnamed cinder cone in the surface.

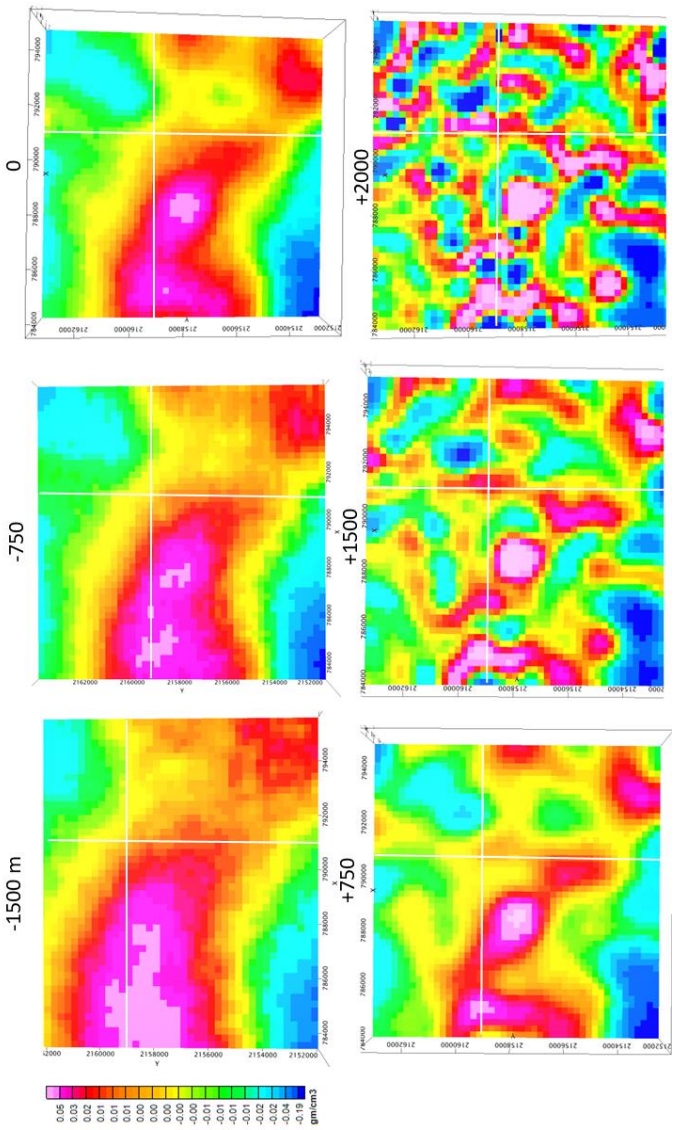


Fig. 15: Horizontal sections of the inverted volume with a 250-m resolution from elevations of -1500 to +2000 m; the density color scale applies to the six sections, coordinates are UTM. Some of the sections appear slightly distorted since they are obtained from a 3D projection (see Section at 0 m); this bears no consequence in the observation of the evolution of the Paricutín anomaly. In every instance, the position of Paricutín volcano is at the intersection of the white lines.

Low-density magma chambers are usually found under volcanic stratovolcanoes (e.g. [28][29][26]) consequently Tancítaro falls into that category; originally, we assumed incorrectly that Paricutín was fed by the Eastern Branch until the higher resolution inversion

was performed. The second conceptual model, corresponding to Paricutín, rests also in the E-W direction embedded in a high-density environment. Figures 14 and 15 revealed the existence of a channel within high-density materials that we recognize as the magma deposit and the conduit that created Paricutin's eruption. The horizontal thickness of the high-density layer separating the magma chamber of Tancítaro from the Paricutín location (see Figure 15) makes it quite difficult to reconcile a connection between them, practically at any depth.

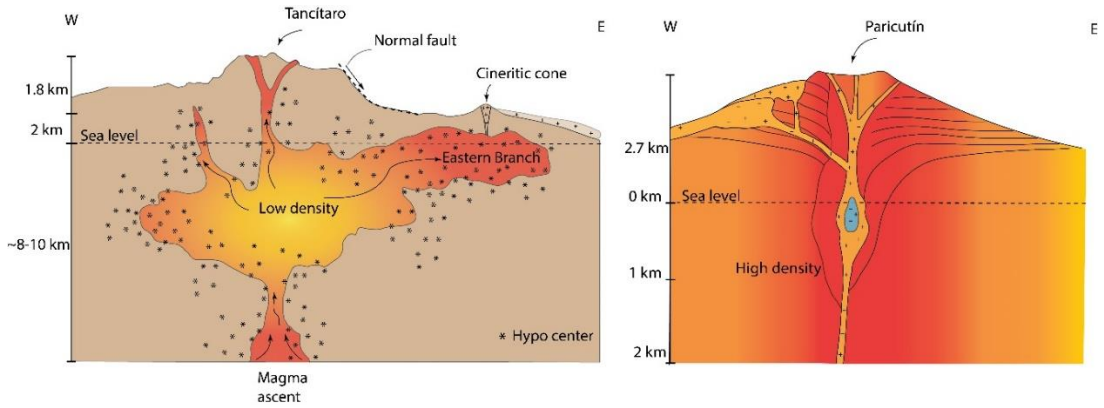


Fig. 16: Conceptual models of the interior of Tancítaro and Paricutín volcanoes, both are oriented in the E-W direction (see Figure 3). Diagrams are along Lines 2051 and 2057 respectively, in Figure 4. a) The outstanding observation in Tancítaro volcano is the existence of the Eastern Branch, b) whilst in Paricutín volcano we located a small, low-density anomaly, at sea level, embedded in a high-density matrix, that we identify with its magma deposit.

DISCUSSION

At sea level, there is an almost circular distribution (Figure 12) of high-density materials enclosing the predominant low-density anomaly in the SW corner of the map, corresponding to Tancítaro volcano. Based on the vertical cross-section in Figure 10, where one or several magma chambers existed north of Tancítaro's summit, in the Paricutín region, and the high-density distribution in Figure 12, we speculate that this region is a magmatic intrusion that preceded the insertion of the low-density Tancítaro anomaly, which was subsequently abandoned, allowing for the solidification of the intruded magmatic products. The compulsion exists to associate these high-density regions with the granitic basement identified by [16] [17]; however, diverse, additional data would be needed to prove it, a task that lies beyond the scope of the present study.

The unexpected observation that Paricutín's eruption was fed through a high-density matrix must be underlined since this is the first observation of its kind and other occurrences may be present in the Tarascan plateau and other volcanic fields. We must note that the spatial resolution (250 m) of the model was crucial to the detection of this conduit, which was not detectable at a resolution of 500 m.

An estimate of the depth of the magma chamber of Paricutín volcano, based on a magnetic model was reported by [30]; they located the feeding chamber at 5 km below sea level. According to the 3D gravity inversion results presented here, a low-density region appearing

under Paricutín is located at sea level (Figure 14), that we identified with a small magma deposit, fed by a vertical conduit. Although the small chamber of Paricutín must have been fed by deeper sources, our models do not show, from -1000 to -6000 m depth, any other signs of a magma chamber under Paricutín.

Another outstanding observation is the detection of the Eastern Branch of the Tancítaro magma chamber, where we identify a lateral flow of magmatic materials towards the east at an angle of ~45º, indicating a considerable concentration of low-density materials at 1800 masl (Figure 7), which seem to indicate a high-risk volcanic region.

From the changes observed in the E-W cross-sections, it appears that TV experienced magmatic intrusions in various directions; some of them resulted in external emissions of volcanic material, whilst others never reached the surface and solidified in those places (e.g., Figure 14).

CONCLUSION

Given the proximity between the Tancítaro stratovolcano and the adjacent Paricutín cinder cone, we decided to examine their structures jointly. Based on satellite-derived, high-resolution gravity data we obtained the Bouguer anomaly over a region containing Tancítaro and Paricutín volcanoes, which was inverted to obtain a 3D density distribution. Several vertical and horizontal cross-sections helped define the distribution of high- and low-density materials in defined volumes that reached 8-10 km depth. Analysis of the 500 m resolution inversion suggested a connection between Tancítaro's low-density magmatic chamber and Paricutín, which turned out to be non-existent.

A second 3D inversion at double the resolution of the former, revealed that the magma chamber of Tancítaro is not connected to Paricutín. Surprisingly, it was determined that the magma deposit and the conduit reaching the surface were embedded in a high-density matrix that in cross-section resembles a solidified magma chamber. The proposed magma chamber of Paricutín can be described as a thin deposit, located at sea level, connected to the surface by up to two conduits. The deep source that fed this small surficial chamber is not detected to depths of ~10 km.

The volume of the low-density anomaly of Tancítaro is surrounded by a high-density formation from the surface to depths of ~6 km, or the bottom of our models, probably continuing downward; this formation shows thicknesses ranging between 4 and 10 km at sea level. Identifying it with the granitic basement of that region is tempting; however, care should be exercised since further geologic and geophysical observations should confirm this question.

References

[1]. Krauskopf, KB (1948) *Mechanism of eruption at Paricutín, México.* Geol. Soc. Am. Bull. 59, (8),711-732. https://doi.org/10.1130/0016-7606(1948)59[711: MOEAPV]2.0.CO;2

[2]. Larrea, P., et al. (2017) *Compositional and volumetric development of a monogenetic lava flow field: The historical case of Paricutin (Michoacán, Mexico)*. J. Volcanol. Geothermal Res., **348,** 36–48. https://doi.org/10.1016/j.jvolgeores.2017.10.016

[3]. Ownby, S., et al., (2007). *Volcán Tancítaro, Michoacán, Mexico, 40Ar/39Ar constraints on its history of sector collapse.* Journal of Volcanology and Geothermal Research, 161(1–2), 1–14. https://doi.org/10.1016/j.jvolgeores.2006.10.009

[4]. Hasenaka, T & Carmichael, ISE (1985) *The cinder cones of Michoacán-Guanajuato, central Mexico, their age, volume and distribution, and magma discharge rate.* J. Volcanol. Geothermal Res. **25**, 105-124.

[5]. Pacheco J, et al., (1999) *Tectonic implications of the earthquake swarm of 1997 in the Michoacan Triangle, Mexico*. J Soc Am Earth Sci, 12:567–577

[6]. Gardine, M., et al., (2011) *Dike emplacement near Parícutin volcano, Mexico in 2006*, Bull Volcanol **73**:123–132, DOI 10.1007/s00445-010-0437-9

[7]. Legrand, D. et al., (2023) *Repeated seismic swarms near Paricutin volcano: precursors to the birth of a new monogenetic volcano in the Michoacán-Guanajuato volcanic field, México?* Bulletin of Volcanology, 85:30. https://doi.org/10.1007/s00445-023-01645-0

[8]. Demant, A. (1978). *Characteristics of the Trans Mexican Volcanic Belt, and its interpretation problems* (In Spanish). In Univ. Nal. Aut. México, Inst. Geología, Revista (Vol. 2, Issue 2, pp. 172–187).

[9]. Ferrari, L., et al., (2012). *The dynamic history of the Trans-Mexican Volcanic Belt and the Mexico subduction zone.* Tectonophysics, 522–523, 122–149. https://doi.org/10.1016/j.tecto.2011.09.018

[10]. Soto, G. L., et al., (2009). *Mantle flow in the Rivera-Cocos subduction zone*. Geophysical Journal International, 179(2), 1004–1012. https://doi.org/10.1111/j.1365-246X.2009.04352.x

[11]. Ferrari, L. (2000). *Advances in the knowledge of the Trans Mexican Volcanic Belt in the last decade* (In Spanish) Boletín de La Sociedad Geológica Mexicana, 53(1), 84–92. https://doi.org/10.18268/BSGM2000v53n1a5

[12]. Gómez-Tuena, A., et al., (2007). *Igneous petrogenesis of the Trans-Mexican Volcanic Belt*. Special Paper of the Geological Society of America, 422(303), 129–181. https://doi.org/10.1130/2007.2422(05)

[13]. Morán-Zenteno, D. J., et al., (2005). *La evolución tectónica y magmática cenozoica del suroeste de México: avances y problemas de interpretación. Boletín de La Sociedad Geológica Mexicana*, 57(3), 319–341. https://doi.org/10.18268/bsgm2005v57n3a4

[14]. Luhr, J.F., and Simkin, T., (1993). *Parícutin. The Volcano Born in a Mexican Cornfield.* Geoscience Press, Phoenix (427 pp).

[15]. Larrea, P., W (2019). *A re-interpretation of the petrogenesis of Paricutin volcano: Distinguishing crustal contamination from mantle heterogeneity.* Chemical Geology, 504 (October 2018), 66–82. https://doi.org/10.1016/j.chemgeo.2018.10.026

[16]. Corona-Chávez et al., (2006). *Asimilación de xenolitos graníticos en el Campo Volcánico Michoacán-Guanajuato: El caso de Arócutin Michoacán, México.* Revista Mexicana de Ciencias Geológicas, **23**(2), 233–245.

[17]. Gómez-Vasconcelos, M. G. (2018). *Paricutín volcano in the Michoacán-Guanajuato volcanic field: a review* (In Spanish). *Ciencia Nicolaita,* 74(August). https://doi.org/https://doi.org/10.35830/cn.v0i74.400

[18]. Delgado T., A. (2022) *Internal structure of Paricutín volcano, using geophysical prospecting methods.* (In Spanish). BA thesis, Escuela Nacional de Estudios Superiores, Unidad Morelia, Morelia, Mich., September, 2022.

[19]. Johnson, C. A., & Harrison, C. G. A. (1990). *Neotectonics in central Mexico.* Physics of the Earth and Planetary Interiors, **64**(2–4), 187–210. https://doi.org/10.1016/0031-9201(90)90037-X

[20]. Wilcox, R. E. (1948). *Activity of Paricutin volcano from April 1 to July 31, 1947.* Transactions, American Geophysical Union, 29(1), 69. https://doi.org/10.1029/TR029i001p00069

[21]. Corona, P. (2002). *Paricutín, One of the twelve Natural Wonders of the World* (In Spanish). 23. http://ce.eng.usf.edu/pharos/wonders/Natural/index.htm

[22]. Hirt, C., et al., (2013). *New ultrahigh-resolution picture of Earth's gravity field.* Geophysical Research Letters, 40(16), 4279–4283. https://doi.org/10.1002/grl.50838.

[23]. Jarvis, A., et al., (2008). *Hole-filled Srtm for the globe Version 4. Available from the CGIAR-CSI SRTM 90m Database*, http://srtm.csi.cgiar.org/.

[24]. Hildenbrand, T. G., et al., (2002). *Rationale and Operational Plan to Upgrade the U S Gravity Database*. USGS Open File Report, 1–12.

[25]. Camacho, M., and Alvarez, R., (2021). *Geophysical Modeling with Satellite Gravity Data: Eigen-6C4 vs. GGM Plus.* Engineering, 13(12): 690 –706. https://doi.org/10.4236/eng.2021.1312050

[26]. Alvarez, R. and Camacho, M. (2023) T*he plumbing system of the Hunga Tonga Hunga Ha'apai volcano,* Journal of Earth Science, Vol. 34, No. 3, p. 706-716, June 2023. https://doi.org/10.1007/s12583-022-1792-0

[27]. Alvarez, R. and Camacho, M. (2023). *Applying High-Resolution Gravity Analysis to Volcanic Plumbing Systems: The Case of Nevado De Toluca Volcano, Mexico.* Transactions on Engineering and Computing Sciences, 11(4). 184-207. https://doi.org/10.14738/tecs.114.15392.

[28]. Alvarez, R. and Yutsis, V. (2015) *Southward migration of magmatic activity in the Colima Volcanic Complex, Mexico: An ongoing process.* International Journal of Geosciences, **6**, 1077-1099. http://dx.doi.org/10.4236/ijg.2015.69085

[29]. Guevara-Betancourt, R., et al., (2023) *Insights into the plumbing system of Colima Volcanic Complex.* Jour. Volcanol. Geothermal Res. 2022 433 (2023) 107711. https://doi.org/10.1016/j.jvolgeores.2022.107711

[30]. López-Loera, H., et al., (2021). *An integrated magnetic survey on lava flows associated to the Paricutin volcano (Western Mexico),* J. South American Earth Sciences, 106 (2021) 103075, https://doi.org/10.1016/j.jsames.2020.103075